Photodissociation Dynamics of Chlorine Peroxide Adsorbed on Ice

S. Inglese, G. Granucci,* T. Laino, and M. Persico

Dipartimento di Chimica e Chimica Industriale, via Risorgimento 35, 56126 Pisa, Italy

Received: December 10, 2004; In Final Form: February 22, 2005

Chlorine peroxide plays an important role in the chlorine−ozone chemistry in the antarctic stratosphere. Adsorption by ice crystals may alter its photochemistry in different ways. We have simulated the photodissociation of a ClOOCl molecule adsorbed on ice by means of a semiclassical representation of the excited state dynamics. Electronic energies and wave functions of ClOOCl are computed by an ad hoc reparametrized semiempirical method, and the interaction with ice is taken into account by a QM/MM strategy. The reaction mechanism is similar to what was previously found for the isolated molecule: sequential or almost simultaneous breaking of both Cl−O bonds leads to the $2Cl + O_2$ reaction products in most cases. The Cl atoms remain temporarily adsorbed on the ice surface, whereas O_2 is ejected. The main effect for the overall chlorine chemistry is probably an increase of the photodissociation rates at long wavelengths, due to the change of adsorption cross sections induced by the interaction with ice.

1. Introduction

The ClO dimer (ClOOCl) is believed to play an important role in the antarctic ozone hole formation, because it is an intermediate in the reversion of ClO radicals to Cl atoms:[1,2]

$$ClO + ClO + M \rightarrow ClOOCl + M \quad (1)$$

$$ClOOCl + h\nu \rightarrow 2Cl + O_2 \quad (2)$$

The photodissociation of the Cl−O bonds, reaction 2, may also occur stepwise

$$ClOOCl + h\nu \rightarrow ClOO + Cl \quad (3)$$

$$ClOO \rightarrow Cl + O_2 \quad (4)$$

A competing process, which generates a null cycle, is

$$ClOOCl + h\nu \rightarrow ClO + ClO \quad (5)$$

Because of its importance in the atmospheric chemistry, numerous research groups, including ours, have been involved in the study of the spectroscopy[3−11] and photochemistry[12−15] of ClOOCl. In previous works we interpreted the absorption spectrum of ClOOCl by ab initio calculations[16] and we simulated the photodissociation of an isolated ClOOCl molecule by the DTSH strategy.[17] As it turns out, the minimum number of states to be considered in a treatment of the photodissociation up to 5 eV is seven. The computed quantum yields and final fragment energies agree with those measured by Moore et al.[13] Little ClO is produced, and only for $h\nu > 4.5$ eV, at the upper end of the explored photon energy range (2.2−5.0 eV). The photodissociation to $2Cl + O_2$ mainly follows the stepwise mechanism at low photon energies, and the simultaneous Cl−O bond breaking at high energies.

The surface of ice particles in the polar stratospheric clouds may accelerate the dimerization reaction and/or adsorb ClOOCl. It has been shown[18] that ClOOCl can react on halide-doped ice surfaces, but adsorption may also affect the photochemistry of ClOOCl in several ways: (a) by causing spectral shifts and changes in the photoabsorption cross sections; (b) by altering the relative yields of 2ClO and $2Cl + O_2$; (c) by inhibiting the photodissociation due to energy transfer to ice and/or desorption; (d) by further interaction of the photodissociation products with the ice surface, after the primary photochemical step.

The aim of this work is to bring out the possible influence of the interaction with ice on the ClOOCl photochemistry and on the mechanism of photodissociation. We are unaware of any previous work, theoretical or experimental, devoted to this topic. The interaction with the ice surface will be modeled using a QM/MM approach which allows us, in principle, to account for all (a)−(d) effects outlined above.

2. Semiempirical Parameters for ClOOCl

The energies and wave functions for ClOOCl were obtained from a MRCI consisting of 232 determinants chosen in a $12e^-$/8MO active space. The CI wave functions were built on molecular orbitals obtained by an SCF with floating occupation numbers[19] (Gaussian width $w = 0.18$ hartree) and a semiempirical reparametrized MNDO/d Hamiltonian was used.

Our previous study of the photodissociation of free ClOOCl was based on PES and wave functions computed by a 6 electron/6 MO CAS-CI, with floating occupation SCF orbitals and a semiempirical Hamiltonian. A suitable reparametrization of the MNDO/d Hamiltonian was used (RMNDO/d). Preliminary simulations of the photodissociation of ClOOCl adsorbed on three layers of water molecules reproducing the Ih ice structure were run with the same CAS-CI and semiempirical parameters, as a first test of the QM/MM procedure employed in this work.[20]

However, the semiempirical treatment setup for the isolated molecule was not well adapted to represent $ClOOCl-H_2O$ interactions. The $6e^-$/6MO CAS-CI allows for a balanced description of states with up to 6 electrons and 6 orbitals in partially filled shells, where a "shell" here means a set of asymptotically degenerate orbitals. For instance, the ClO + ClO asymptote, with two π^* shells, each containing 3 electrons, is correctly described. So is the ClOO + Cl dissociation (6 electrons and 4 orbitals) and the $Cl_2 + O_2$ one (2 electrons in 2 orbitals). Instead, the $2Cl + O_2$ fragmentation is characterized

10.1021/jp044368k CCC: $30.25
Published on Web 03/30/2005

TABLE 1: Target Values for the Optimization of Semiempirical Parameters and Corresponding Values at Semiempirical Level[a]

	RMNDO/d (ref 17)	RMNDO/d−W (this work)	target
ClOOCl Dipole (debye)			
equilib geometry	−1.763	1.035	0.539
$R_{OCl} = 2.01$	−2.370	0.066	0.305
$R_{OCl} = 2.64$	−0.176	−0.920	−0.288
$R_{OCl} = 4.23$	0.001	−0.023	−0.077
Energies Referred to ClOOCl at Equilibrium			
ClO + ClO	0.95	0.55	0.74[b]
$Cl_2 + O_2$	−0.45	−0.38	−0.36[b]
O_2 + 2Cl		0.87	1.17[b]
Cl + ClOO	0.24	1.09	0.82[b]
E_{cis}	0.59	0.50	0.44[c]
E_{trans}	0.14	0.09	0.23[c]
ClO + Cl + O		3.58	3.61[d]
Geometries			
ClOOCl			
O−O	1.317	1.512	1.426[e]
O−Cl	1.767	1.865	1.704[e]
∠ClOO	109.486	109.976	110.100[e]
∠ClOOCl	104.491	106.542	81.000[e]
ClOO			
O−O	1.181	1.350	1.201[f]
O−Cl	1.818	2.004	2.139[f]
∠ClOO	111.478	112.158	115.700[f]
ClO			
O−Cl	1.689	1.802	1.570[g]

[a] Energies in eV, distances in Å, angles in degrees. Unless otherwise specified, all the target values were obtained with the ab initio CAS-CI method of ref 17. [b] See refs 3, 21, 22, and 23. [c] See ref 24. [d] Inferred from G2 calculations of Li and Ng;[25] this value was not included in the target function for parameter optimization. [e] See ref 26. [f] See ref 27. [g] See ref 21.

by 12 electrons and 8 orbitals in partially filled shells, which is beyond the capability of the $6e^-$/6MO CAS-CI. In fact, in the simulation of the free molecule dissociation, we stopped the trajectories before both Cl−O distances were too large. As a consequence of the particular CI space employed in that study the importance of the ionic configurations was overestimated, because they replaced the missing neutral ones in the description of the lowest electronic states. In particular, the polarity of the Cl−O bonds in the ground state was reversed in this semiempirical calculation with respect to the ab initio ones: $Cl^- - O^+$ instead of $Cl^+ - O^-$. Of course this feature cannot be ignored when ClOOCl−water interactions are considered.

We have therefore expanded the MO active space to $12e^-$/8MO, selecting 232 determinants that are needed to represent correctly all the dissociation limits. With these wave functions, the semiempirical parameters were re-optimized, using the same technique exploited in our previous work.[17] The target values to be reproduced this time included also the molecular ground-state dipole for different symmetric elongations of both Cl−O bonds, computed with the same ab initio method previously used for the PES[17] (CAS-CI with 26 electrons in 16 MOs; Ahlrichs VTZ plus polarization Gaussian basis set). The results of the optimization are shown in Table 1 and in Figures 1−4. The new set of parameters, labeled RMNDO/d−W, is shown in Table 2. As one can see from Table 1, the new set of parameters yields the right polarity for the Cl−O bonds, at least qualitatively. In a neighborhood of the ground state equilibrium geometry, the potential energy curves shown in Figures 1−4 are similar to those previously obtained with the RMNDO/d parameter set.[17] However, in this case we get the right degeneracies for the three body fragmentation O2 + 2Cl and the dissociation energies are better reproduced[31] (see also Table 1). The peroxide and Cl−O bonds obtained with the RMNDO/d−W parameter set are too long by respectively 0.09 and 0.16 Å. However, the changes in equilibrium bond lengths of a leaving group (ClOO, ClO or O_2) with respect to ClOOCl are similar to those obtained with the ab initio calculations.[17,31]

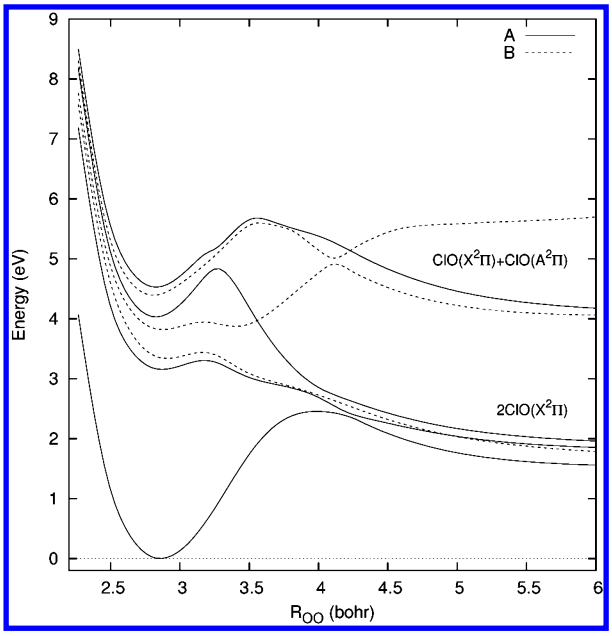

Figure 1. Dissociation curves to 2ClO in a vacuum. The O−O distance is varied; all the other coordinates are fixed to the optimized equilibrium values. The labels indicate the symmetry of the electronic states.

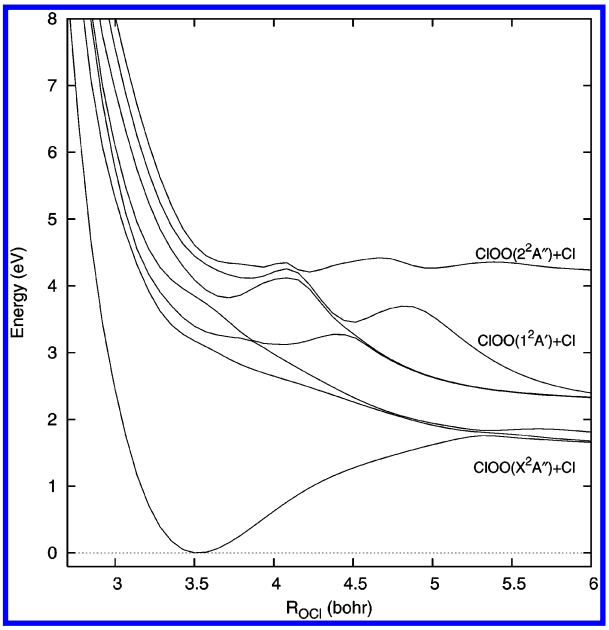

Figure 2. Dissociation curves to ClOO + Cl in a vacuum. The Cl−O distance is varied; all the other coordinates are fixed to the optimized equilibrium values.

To summarize, it is evident that the good quality of the RMNDO/d PESs is kept, with some improvements (polarity of the Cl−O bonds, dissociation energies). A photodissociation dynamics calculation with the RMNDO/d−W parameter set in a vacuum yields results comparable with the RMNDO/d set.[17] The main difference concerns the quantum yield for the 2ClO dissociation channel (Φ_{ClO}): although our previous results gave $\Phi_{ClO} > 0$ (in particular $\Phi_{ClO} = 0.05$) only for the high excitation energies (4.4−5.0 eV), with the present calculations we obtain a nonzero quantum yield for 2ClO ($\Phi_{ClO} = 0.11$) only in the

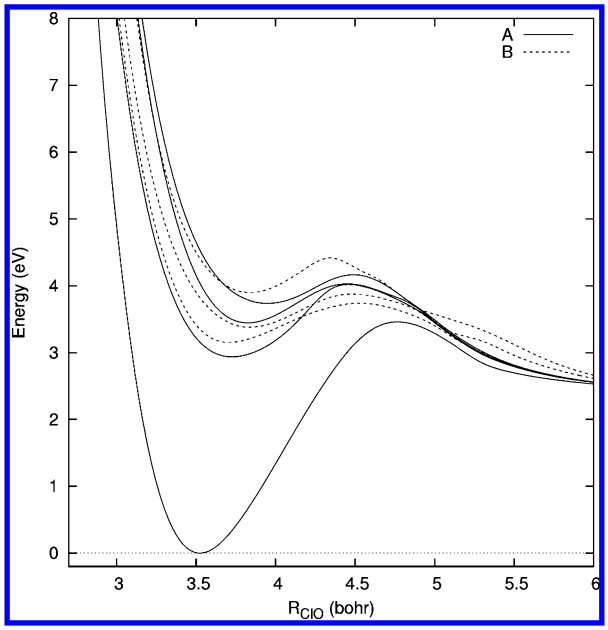

Figure 3. Dissociation curves to $2Cl + O_2$ in a vacuum. Both Cl−O distances are varied symmetrically, all the other coordinates are fixed to the optimized equilibrium values. The labels indicate the symmetry of the electronic states.

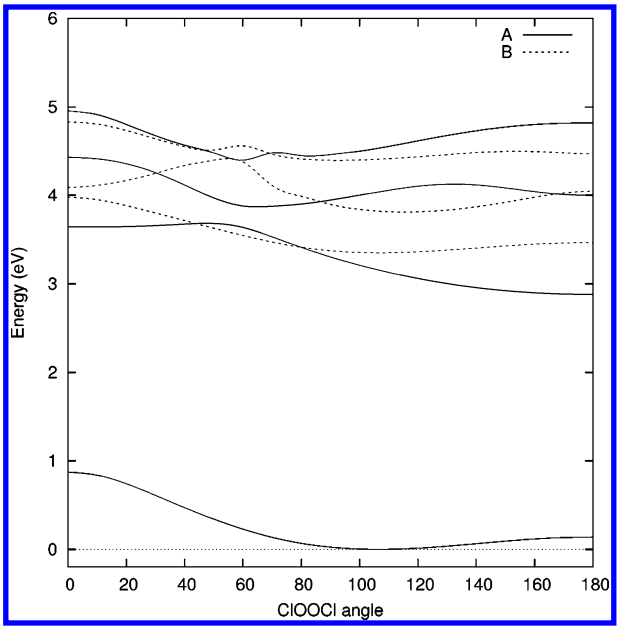

Figure 4. Torsion curves along the dihedral angle ClOOCl (in a vacuum). All the other coordinates are fixed to the optimized equilibrium values. The labels indicate the symmetry of the electronic states.

case of low excitation energy (2.8−3.5 eV). This last result is in agreement with very recent experimental findings.[15]

The interaction of ClOOCl with water was modeled with a QM/MM scheme in which the water molecules are treated at the Molecular Mechanics level.[20,32] For the MM representation of the water molecule we adopted the flexible SPC model.[33] We introduced Lennard-Jones (LJ) interactions between the water atoms and the QM subsystem, keeping for water O the LJ parameters of the SPC model and optimizing the LJ parameters of H (water), Cl and O (ClOOCl) to reproduce ab initio results for the ClOOCl−H_2O complex.

The reference ab initio data were provided by MP2/6-311G** calculations for the ClOOCl−H_2O supermolecule, run with three different relative orientations of the two molecules: one is representative of H(water)−O(ClOOCl) interactions, and two

TABLE 2: Original[28,29] MNDO/d and Reoptimized RMNDO/d−W Parameters for Oxygen and Chlorine[a]

	O		Cl	
parameters	MNDO/d	RMNDO/d−W	MNDO/d	RMNDO/d−W
U_s	−99.64	−119.96	−69.62	−80.56
U_p	−77.80	−86.38	−59.10	−60.54
U_d			−36.67	−30.39
β_s	−32.69	−30.06	−6.037	−5.672
β_p	−32.69	−35.74	−19.18	−19.76
β_d			−1.878	−1.908
ξ_s	2.700	1.893	2.562	2.324
ξ_p	2.700	2.483	2.389	2.162
ξ_d			1.251	1.108
α_A	3.161	2.833	2.180	1.963
ξ_{sN}			1.881	1.652
ξ_{pN}			1.181	1.429
ξ_{dN}			1.141	0.838
G_{ss}	15.42	23.20	13.21	12.153
G_{sp}	14.48	13.55	9.419	5.287
G_{pp}	14.52	13.96	8.996	8.377
G_{p2}	12.98	11.84	7.945	6.171
H_{sp}	3.940	7.217	3.081	2.941
K_1	0.000	0.053	0.000	0.010
L_1		4.652		3.592
M_1		1.318		1.219
K_2	0.000	−0.034	0.000	−0.010
L_2		6.394		4.714
M_2		1.591		2.476

[a] For the meaning of the parameters see the MOPAC manual.[30]

of O(water)−Cl(ClOOCl) interactions (see Figure 5). Constrained geometry optimizations were preferred to the determination of true minima, because when ClOOCl approaches the ice surface it interacts with water molecules in several relative orientations, possibly very different from the optimal one for a single water molecule. The constraints imposed in the geometry optimizations are (see Figure 5): (A) the water molecule is kept fixed in the Cl−O−O plane; (B) the plane of the water molecule is kept perpendicular to the Cl−O−O plane; (C) the OH (H_2O) and O (ClOOCl) are kept on a straight line and the OH is on the Cl−O−O plane. The results of the optimization are shown in Tables 3 and 4.

3. Preparation of an Ice Crystal and Adsorption of ClOOCl

The ClOOCl−ice system was made up in three steps.

Step 1: optimize a cluster of 216 water molecules in three layers, with periodic geometry constraints corresponding to the Ih crystal structure. This is probably the most stable ice structure in the conditions of the antarctic stratosphere ($T \simeq 190$ K), although little is known about the real structure of the surface of the ice crystals which form the SPC's (stratospheric polar clouds).[1,2] The ice slab we obtain has the dimensions of 25 × 25 × 10 Å, with alternate rows of H and O atoms sticking out of the upper and lower surfaces.

Step 2: fix the position of all atoms in the bottom and side layers, and optimize the remaining 64 water molecules without other constraints. This step replaces the symmetry constraints of step (1) with other constraints that can be applied also after adding the ClOOCl adsorbate. Constraints of either type are needed to keep an approximately planar ice surface, as would occur in the presence of a semi-infinite (or very large) crystal. Without constraints, a small cluster with or even without adsorbate would change its shape to a more compact one, the most stable being probably approximately spheroidal.

Step 3: add ClOOCl on top of the ice slab and run a brownian dynamics for 40 ps, with the temperature of 190 K. During the

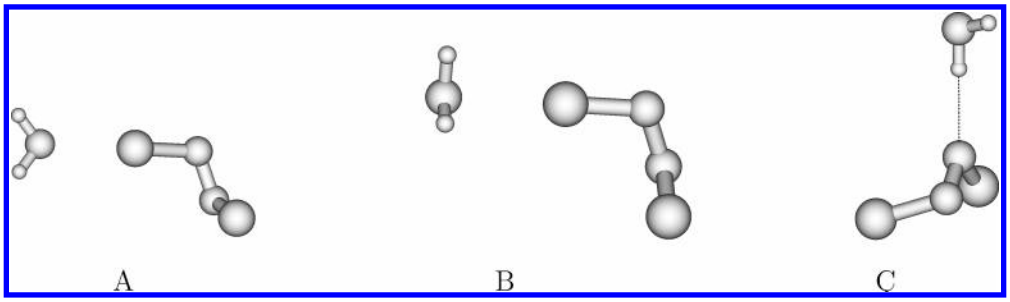

Figure 5. ClOOCl−H_2O relative orientations considered in the optimization of the Lennard-Jones MM parameters.

TABLE 3: Interaction Energies and Geometrical Parameters for ClOOCl−H_2O Complex[a]

	QM/MM	MP2/6-311G**
	Interaction Energy (eV)	
A	0.212	0.210
B	0.207	0.207
C	0.093	0.093
	Intermolecular Distance (Å)	
A (Cl−O)	2.708	2.676
B (Cl−O)	2.672	2.749
C (O−H)	2.330	2.120

[a] Labels A−C refer to Figure 5.

TABLE 4: Lennard-Jones MM Parameters

atom	σ (Å)	ϵ (kcal/mol)
O (H_2O)	3.1655[a]	0.1554[a]
H (H_2O)	1.6327[b]	0.7554[b]
O (ClOOCl)	4.2360	0.00162
Cl (ClOOCl)	2.0584	20.4779

[a] SPC parameters. [b] Only used for interaction with ClOOCl.

first several picoseconds one observes an almost steady decrease of the potential energy, whereas the ClOOCl molecule accommodates in a "groove" of the ice surface. When this process ends, the positions of ClOOCl and H_2O atoms undergo relatively smaller fluctuations. The Cl atoms of ClOOCl point the bottom of the groove and the O atoms point outward. The internal coordinates of ClOOCl where only slightly altered with respect to the isolated molecule (C_2 geometry with a ClOOCl dihedral angle of about 90°). The ClOOCl−ice system is shown in Figure 6.

4. Photodissociation Dynamics

The simulation of the photodissociation dynamics was carried out with the same DTSH method previously used for the study of the ClOOCl photodynamics in a vacuum.[17] Six excited states fall within the considered energy range and give place to three distinct features (maxima or shoulders) in the absorption spectrum. Both ab initio[16] and semiempirical calculations (see Figure 7) reproduce well such features of the experimental spectrum. Therefore we ran three swarms of trajectories, with different ranges of excitation energies: $\Delta E = 2.8-3.5$, 3.5−4.0, and 4.0−5.0 eV. The initial conditions (nuclear coordinates and momenta, and electronic state) were sampled according to the following algorithm. A number of points are chosen, at regular time intervals, along the brownian trajectory (see previous section). For each point, one or more attempts to start a trajectory by vertical excitation are made. The number of attempts M depends on an arbitrary value f_r, which is a reference oscillator strength. The algorithm takes into account the N_x electronic states with excitation energies $\Delta E_i = U_i - U_0$ (potential energy difference with respect to the ground state, at the given geometry) falling within the wanted energy range. If

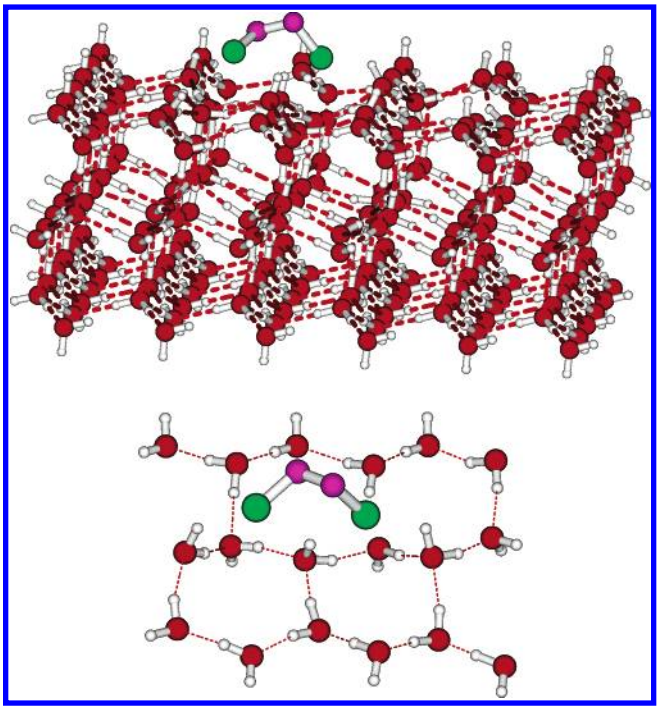

Figure 6. ClOOCl−ice system. Bottom panel: only a few water molecules near to ClOOCl are shown. Top panel: the whole system is shown.

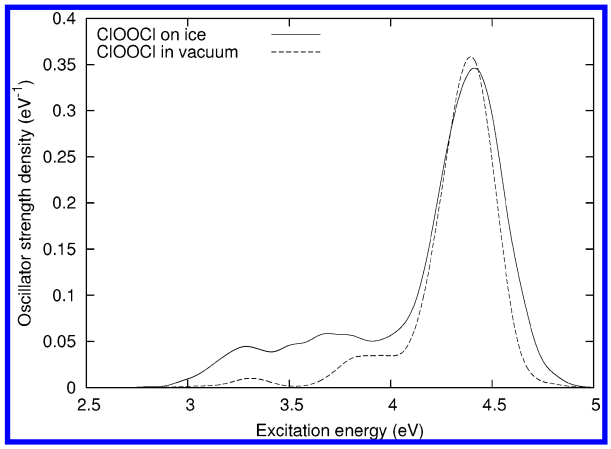

Figure 7. Spectra computed from brownian trajectories for ClOOCl on ice (solid line) and in a vacuum (dashed line). In both cases the temperature was 190 K.

none is found ($N_x = 0$), no trajectory is started with the current coordinates and momenta. If $N_x > 0$, the oscillator strengths f_i of the N_x states are computed. Next, we compare f_r with the sum of the f_i and we take the smallest integer M such that $Mf_r > \sum f_i$. Finally, for M times, we select at random one of the N_x excited states to start a trajectory. The selection algorithm is such that state i has a probability f_i/f_r to be chosen, and there is

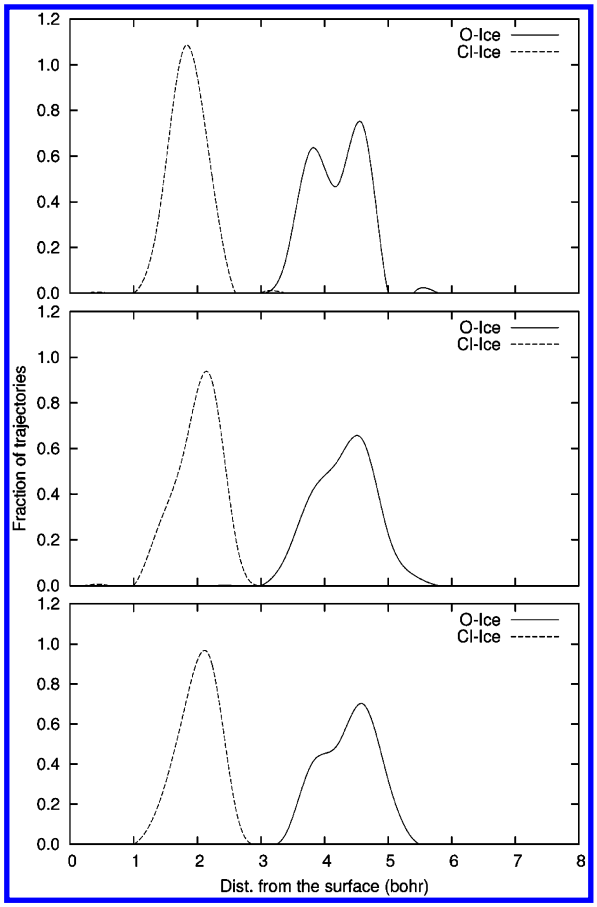

Figure 8. Initial distance of Cl and O atoms from the ice surface. Bottom panel: excitation energy in the range 2.8−3.5 eV. Medium panel: excitation energy in the range 3.5−4.0 eV. Top panel: excitation energy in the range 4.0−5.0 eV.

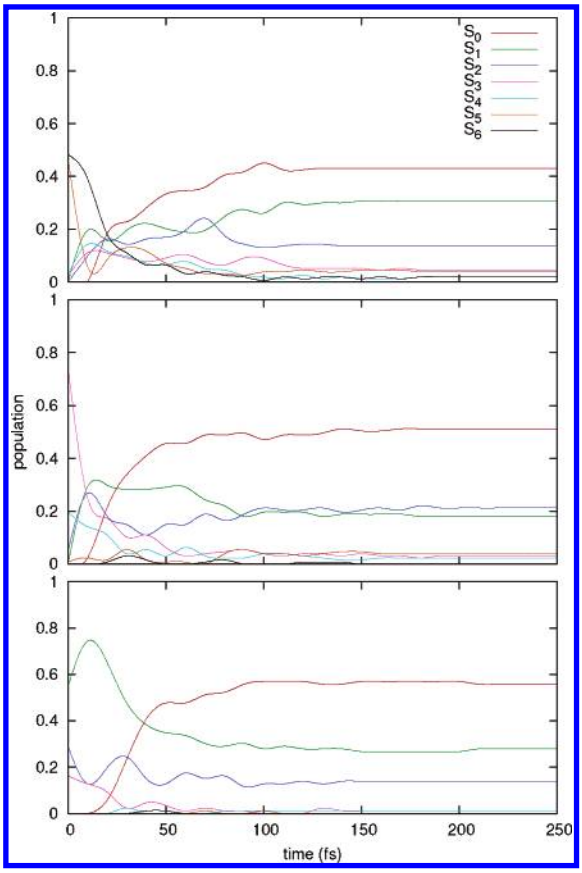

Figure 9. Average state populations. Bottom panel: excitation energy in the range 2.8−3.5 eV. Medium panel: excitation energy in the range 3.5−4.0 eV. Top panel: excitation energy in the range 4.0−5.0 eV.

also a probability $M - \sum f_i/f_r$ that no excitation takes place, so that in the end less than M trajectories may start from the current starting point. According to our selection algorithm, the trajectories actually started were 85 for $\Delta E = 2.8-3.5$ eV, 127 for 3.5−4.0 eV and 153 for 4.0−5.0 eV. The integration time step was 0.1 fs.

Figure 8 yields information about the average position and orientation of the adsorbate with respect to the ice surface, for each excitation energy interval. We arbitrarily defined a plane, representative of the surface, by choosing three O atoms at three corners of the upper layer of water molecules, with ClOOCl approximately in the middle. Let z be an axis perpendicular to the plane, and pointing out of the ice slab. In the figure we report the distribution of z coordinates of O and Cl atoms of ClOOCl at the beginning of the three swarms of trajectories. The initial positions reveal that ClOOCl is oriented with "inner" Cl atoms and one O atom sticking out of the surface definitely more than the other one. In fact, the distribution of z coordinates is unimodal for the Cl atoms and bimodal for the O ones. The distributions for the two lower energy intervals show some minor difference with respect to the other one: in particular, for the O atoms we see a single peak with a shoulder rather than two distinct peaks. Such a difference can only derive from the algorithm of selection of initial coordinates (and momenta), which acts, for all energy intervals, on the same database of phase space points generated by the brownian motion. One should recall that the oscillator strength associated with the first four excited singlets is small if compared with that of S_5 and S_6,[16] so for the lower excitation energy ranges the algorithm may favor structures rather far from the equilibrium one, such that the oscillator strength is larger because of the geometrical distortion of the adsorbate and/or because of the interactions with water molecules. In fact, the spectrum generated by brownian sampling of the nuclear geometries (see Figure 7) shows that in the two lower energy interval the oscillator strength is increased (by 4 times for $\Delta E = 2.8-3.5$ eV) with respect to the isolated molecule. In the highest excitation energy interval, where the gas-phase oscillator strength is much larger, this effect is less important.

Peterson and Francisco[11] show the existence of two low-lying triplet states (about 0.9 eV below the first excited singlet) with non-negligible oscillator strengths due to spin−orbit coupling. Because these absorption are about 1 order of magnitude weaker than the lowest singlet feature and inevitably overlap with it, due to the dissociative nature of the states, we do not expect relevant modifications of our results due to neglecting the triplet absorption. The presence of triplet states can also modify the dynamics because of singlet−triplet nonradiative transitions. Because the shape of the PES for the triplet states of ClOOCl is unknown, their influence on the nonadiabatic dynamics cannot be assessed. Note that, assuming a singlet−triplet coupling strength of the order of the atomic spin−orbit coupling constant of Cl ^{2}P (about 590 cm^{-1}), we estimate a time for the intersystem crossing of about 30 fs. Therefore singlet−triplet transitions could in fact occur, even in the short time of a direct dissociation act. However, such transitions are most probable at medium or large distances, where the singlet and triplet curves must be closer and almost parallel, thus giving place to the same dissociation mechanism.

Figure 9 shows the average state populations for the three swarms of trajectories. One can see that the initial states, to which vertical excitation is made, are mainly S_1, S_2, S_3 in the

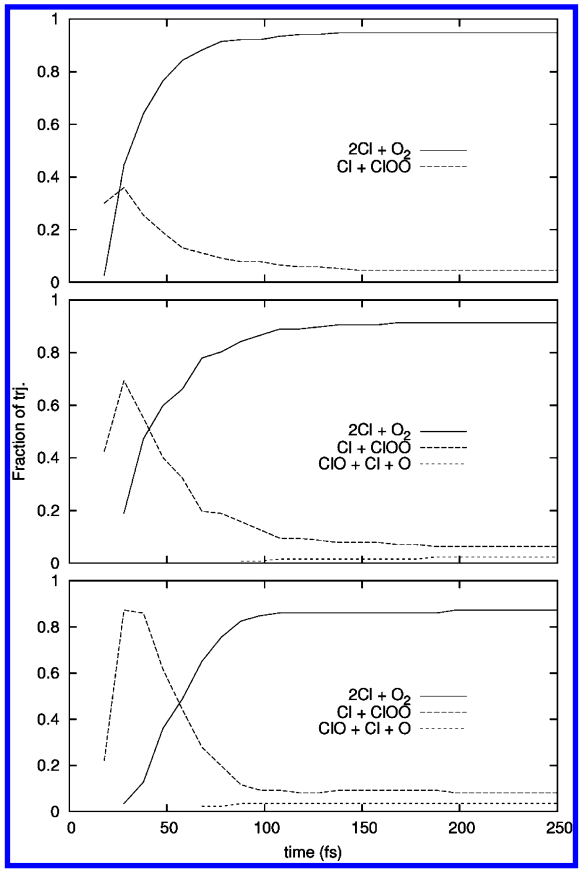

Figure 10. Reaction products. Bottom panel: excitation energy in the range 2.8−3.5 eV. Medium panel: excitation energy in the range 3.5−4.0 eV. Top panel: excitation energy in the range 4.0−5.0 eV.

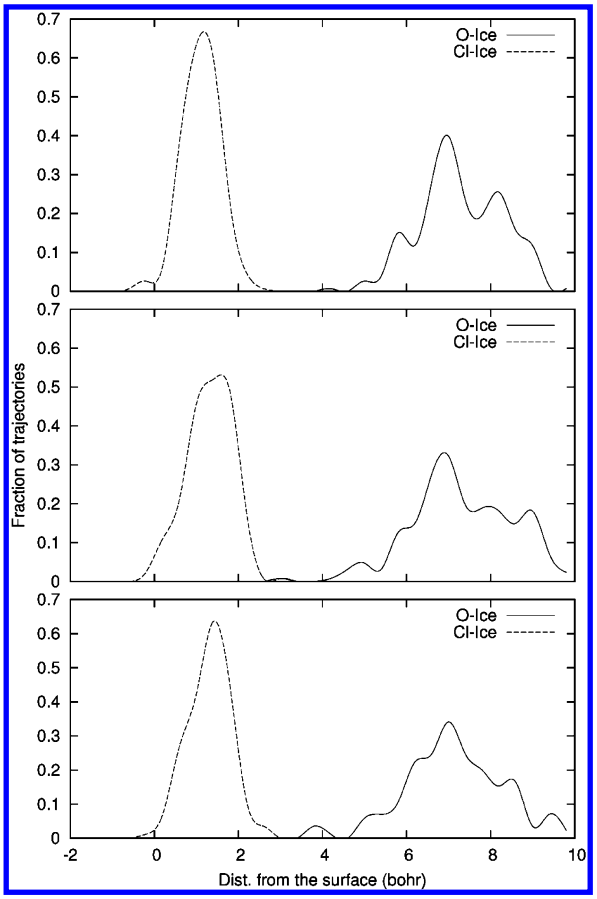

Figure 11. Final distance of Cl and O atoms from the ice surface. Bottom panel: excitation energy in the range 2.8−3.5 eV. Medium panel: excitation energy in the range 3.4−4.4 eV. Top panel: excitation energy in the range 4.0−5.0 eV.

low energy interval, S_3, S_4 in the medium one, and S_5, S_6 in the high one. As in the gas phase dynamics, very fast nonadiabatic transitions to lower states take place during the dissociation, and a number of states are populated at the end (most of them being asymptotically degenerate).

We adopted throughout the following stopping conditions: (1) if both $R_{ClO} > 8$ bohr and $R_{Cl'O'} > 8$ bohr, the trajectory ends with the production of $2Cl + O_2$; (2) if $R_{ClO} > 10$ bohr and $R_{Cl'O'} < 8$ bohr (or vice versa), the trajectory ends with the production of $ClOO + Cl$; (3) if $R_{OO} > 8$ bohr, the trajectory ends with the production of 2ClO (actually, we never observed this outcome). However, to monitor the transient production of the ClOO radical, and the possible asymmetric character of the fragmentation mechanism, we plotted in Figure 10 the fraction of trajectories found at any time in one of the possible dissociation channels. To this aim, we define a bond as dissociated if its length overcomes 4.5 bohr.

In the low and medium excitation energy ranges a small but non negligible fraction of trajectories (4% and 3%, respectively) give rise to $ClO + Cl + O$. Note that, according to the dissociation energies shown in Table 1, this channel is not even accessible in the gas phase with excitation energy in the low range ($\Delta E = 2.8-3.5$ eV) and in fact we did not observe such kind of dissociation for the isolated molecule. Apart from the minor channel $ClO + Cl + O$ and according to the above definition, with low energy excitation most trajectories remain for a short time (50−100 fs) in the $ClOO + Cl$ region and then progress toward full fragmentation ($2Cl + O_2$ region). The total time required for the full fragmentation is of the order of 150 fs. In the end, according to our rule on the bond lengths, we have 88% $2Cl + O_2$ and 8% $ClOO + Cl$. Given the small barrier opposing ClOO dissociation in the ground state, the probable fate of ClOO is to produce $Cl + O_2$ in a longer time scale. However, the dissociation mechanism is clearly sequential at low excitation energies. As in the case of the isolated molecule, with higher energies the permanence in the $ClOO + Cl$ region is shorter and the mechanism is most appropriately described as simultaneous but asymmetric dissociation of the two Cl−O bonds. The final outcome for $\Delta E = 3.5-4.0$ eV is 91% $2Cl + O_2$ and 6% $ClOO + Cl$, whereas in the high energy range 95% $2Cl + O_2$ and 5% $ClOO + Cl$.

TABLE 5: Energy Disposal for the O_2 Fragment (eV)

excitation energy range	total absorbed energy	E_{trasl}	E_{rot}	E_{vib}
2.8−3.5	3.24	1.31	0.15	0.33
3.5−4.0	3.77	1.63	0.23	0.19
4.0−5.0	4.40	1.62	0.23	0.37

Another kind of information about the fate of the photodissociation fragments is found in Figure 11. Here we show the final positions of the O and Cl atoms with respect to the conventional surface plane. The recoil momentum due to bond breaking pushes the Cl atoms even more inside the ice crystal, with a broadening of the distribution of z coordinates for all the energy ranges. The Cl atoms therefore remain adsorbed on the ice surface and will obviously transfer their kinetic energy to the crystal lattice. The O_2 molecule, on the contrary, flies away. Its initially bimodal distribution broadens and gets more complicated. The energy disposal for the O_2 fragment is shown in Table 5, only for the trajectories giving rise to a synchronous dissociation (the above referred stop condition 1). The O_2 fragment takes about a half of the excitation energy, mainly as translational energy.

The recoil momentum of the two Cl atoms pushes them in opposite directions: no formation of Cl_2 occurs in our trajectories. About their fate, one may envisage three possibilities: (1) desorption as Cl atoms; (2) migration on the ice surface and recombination to form Cl_2, which is subsequently desorbed; (3) disproportionation: $2Cl + H_2O \rightarrow HCl + HOCl$. Only the last reaction would effectively subtract Cl atoms from the ozone-destroying cycles, because HCl and HOCl, thanks to their strong affinity for water ice, may be eliminated with precipitations.

5. Conclusions

The conclusions we can draw from the simulations of the photodissociation of ClOOCl adsorbed on ice, described in the previous sections, are subject to important caveats. These concern the real structure of the surface of the stratospheric ice crystals, which is largely unknown: we simply made a reasonable assumption, on the basis of the relative stability of the different crystal structures, and allowed for a certain degree of freedom by running brownian dynamics after inserting ClOOCl at interaction distance. The brownian motion of ClOOCl itself yields one basic orientation of the molecule with respect to the ice crystal, which deeply affects the photodissociation dynamics. We cannot exclude that a much longer brownian trajectory, or a different starting point, would not reveal the existence of different (but probably less stable) absorption sites and orientations.

The results of the simulations lead to simple conclusions about the influence of ice adsorption on the photodissociation dynamics and on the overall chlorine photochemistry in the stratospheric clouds. The mechanism of photodissociation is basically the same as in gas phase: the two Cl−O bonds are broken, not simultaneously but with little delay; only at low excitation energies the formation of (mostly transient) ClOO radical is obtained. Both the ClOO and the much more abundant 2Cl photodissociation products remain adsorbed on the ice surface, which also receives a large fraction of the available photon energy. No desorption of ClOOCl as a whole occurs, whereas an O_2 molecule is set free. The O−O bond breaking occurs with low quantum yield as in the free molecule photolysis but in this case is always accompanied by a Cl−O bond dissociation.

The main effect of practical importance will probably be the increase of the adsorption cross section at low excitation energies (2.8−3.5 eV, corresponding to wavelengths of 350−440 nm), due to ClOOCl−water interactions: in fact, in this spectral region the solar photon flux is many times stronger than at shorter wavelengths.[1,2] Stabilization of the Cl adsorption on ice by disproportionation to HCl and HOCl may also affect the overall chlorine cycle.

References and Notes

(1) Seinfeld, J. H.; Pandis, S. N. *Atmospheric chemistry and physics*; J. Wiley & Sons: New York, 1998.

(2) Sander, S. P.; Friedl, R. R.; Ravishankara, A. R.; Golden, D. M.; Kolb, C. E.; Kurylo, M. J.; Huie, R. E.; Orkin, V. L.; Molina, M. J.; Moortgat, G. K.; Finlayson-Pitts, B. J. *Chemical Kinetics and Photochemical Data for Use in Atmospheric Studies*; JPL Publication 02-25; Jet Propulsion laboratory: Pasadena, CA.

(3) Cox, R. A.; Hayman, G. D. *Nature* **1988**, *332*, 796.

(4) Permien, T.; Vogt, R.; Schindler, R. N. Mechanisms of Gas Phase-Liquid-Phase Chemical Transformations. In *Air Pollution Report #17*; Cox, R. A., Ed.; Environmental Research Program of CEC: Brussels, 1988.

(5) De More, W. B.; Tschuikow-Roux, E. *J. Phys. Chem.* **1990**, *94*, 5856.

(6) Burkholder, J. B.; Orlando, J. J.; Howard, C. J. *J. Phys. Chem.* **1990**, *94*, 687.

(7) Huder, K. J.; De More, W. B. *J. Phys. Chem.* **1995**, *99*, 3905.

(8) Jensen, F.; Oddershede, J. *J. Phys. Chem.* **1990**, *90*, 2235.

(9) Stanton, J. F.; Bartlett, R. J. *J. Chem. Phys.* **1993**, *98*, 9335.

(10) Tomasello, P.; Ehara, M.; Nakatsuji, H. *J. Chem. Phys.* **2002**, *116*, 2425.

(11) Peterson, K. A.; Francisco, J. S. *J. Chem. Phys.* **2004**, *121*, 2611.

(12) Molina, M. J.; Colussi, A. J.; Molina, L. T.; Schindler, R. N.; Tso, T.-L. *Chem. Phys. Lett.* **1990**, *173*, 310.

(13) Moore, T. A.; Okumura, M.; Seale, J. W.; Minton, T. K. *J. Phys. Chem.* **1999**, *103*, 1691.

(14) Kaledin, A. L.; Morokuma, K. *J. Chem. Phys.* **2000**, *113*, 5750.

(15) Plenge, J.; Flesch, R.; Kühl, S.; Vogel, B.; Müller, R.; Stroh, F.; Rühl, E. *J. Phys. Chem. A* **2004**, *108*, 4859.

(16) Toniolo, A.; Persico, M.; Pitea, D. *J. Phys. Chem. A* **2000**, *104*, 7278.

(17) Toniolo, A.; Granucci, G.; Inglese, S.; Persico, M. *PhysChemChemPhys* **2001**, *3*, 4266.

(18) De Haan, D. O.; Birks, J. W. *J. Phys. Chem. A* **1997**, *101*, 8026.

(19) Granucci, G.; Toniolo, A. *Chem. Phys. Lett.* **2000**, *325*, 79.

(20) Persico, M.; Granucci, G.; Inglese, S.; Laino, T.; Toniolo, A. *J. Mol. Struct. THEOCHEM* **2003**, *621*, 119.

(21) Huber, K. P.; Herzberg, G. *Constants of Diatomic Molecules*; Van Nostrand: New York 1979.

(22) Basco, N.; Hunt, J. E. *Int. J. Chem. Kinet.* **1979**, *11*, 649.

(23) Chase, M. W., Jr.; Davies, C. A.; Downey, J. R., Jr.; Frurip, D. J.; McDonald, R. A.; Syverud, A. N. *J. Phys. Chem. Ref. Data* **1985**, *14*, suppl. 1.

(24) Gómez, P. C.; Pacios, L. F. *J. Phys. Chem.* **1996**, *100*, 8731.

(25) Li, W.-K.; Ng, C.-Y. *J. Phys. Chem. A* **1997**, *101*, 113.

(26) Birk, M.; Friedl, M. M.; Cohen, E. A.; Pickett, H. M.; Sander, S. P. *J. Chem. Phys.* **1989**, *91*, 6588.

(27) Peterson, K. A.; Werner, H.-J. *J. Chem. Phys.* **1992**, *96*, 8948.

(28) Dewar, M. J. S.; Thiel, W. *J. Am. Chem. Soc.* **1977**, *99*, 4899.

(29) Thiel, W.; Voityuk, A. A. *Int. J. Quantum Chem.* **1992**, *44*, 807.

(30) Stewart, J. J. P. *MOPAC 98 Manual*; Fujitsu Limited: Tokyo, Japan, 1999.

(31) Errata corrige in ref 17: (a) Table 4 and Figure 2, the S_6 state of ClOOCl correlates to ClOO($2\ ^2A''$) + Cl (^2P); (b) bond variations ΔR_{ClO}, ΔR_{OO} are given in angstroms, not bohr (p 4271).

(32) Toniolo, A.; Ciminelli, C.; Granucci, G.; Laino, T.; Persico, M. *Theor. Chem. Acc.* **2004**, *111*, 270.

(33) Dang, L. X.; Pettitt, B. M. *J. Phys. Chem.* **1987**, *91*, 3349.